ISSN 1846-6168 (Print), ISSN 1848-5588 (Online)
https://doi.org/10.31803/tg-20240925082150

Original scientific paper
Received: 2024-09-25, Accepted: 2024-12-04

SurfaceVision: An Automated Module for Surface Fault Detection in 3D Printed Products

Laukesh Kumar*, Manoj Kumar Satyarthi

Abstract: In the era of Industry 4.0, the advent of 3D printing has revolutionized manufacturing by significantly reducing financial and time efforts. 3D printed products are created layer-by-layer based on digital Computer Aided Design (CAD) inputs, yet they remain susceptible to defects that can compromise quality. Detecting these layerwise faults is important to ensure high quality outputs. The traditional method currently requires visual information processing devices or continuous monitoring of the process via a camera, which is very resource consuming and costly. Machine learning techniques being used for automatic detection of the faults suffer in real time conditions with inefficient fault detection due to the inability of adaptation to real time changes in the printing process. Along with the inability to assess layer by layer protrusion development, the current ML techniques are lacing in 3D printing fault detection. This paper introduces SurfaceVision, an automated system for surface fault detection in 3D printed products, leveraging the ResNet-18 architecture as the backbone. Our framework utilizes a combination of contrastive learning and multi domain loss function to identify and classify defects with high accuracy. Comparative experiments demonstrate that the ResNet-18 based SurfaceVision outperforms the baseline.

Keywords: 3D printing; deep learning; quality control; real-time monitoring; ResNet-18; surface fault detection

1 INTRODUCTION

In the era of Industry 4.0, 3D printing, also known as Additive Manufacturing (AM), has revolutionized manufacturing by enabling the layer-by-layer creation of complex products based on digital designs. Among the seven main categories of AM technologies classified by the ASTM F42/ISO TC 261 standard, this study specifically focuses on Material Extrusion (MEX) technologies, which include widely used processes such as Fused Deposition Modelling (FDM) and Fused Filament Fabrication (FFF). These MEX technologies are particularly popular in industrial and consumer applications due to their affordability and accessibility [1]. However, they are also prone to defects like layer misalignment, surface roughness, and incomplete layers, which can compromise product quality [2]. The presence of these defects/flaws reduces the functionality and aesthetics of the resultant product [3].

Therefore, rectifying these flaws is imperative to ensure quality of the manufactured product. Traditional ways of identifying these flaws rely on manual inspection or rudimentary automated systems, often lacking the necessary accuracy or speed to finish the task. [4]. Fig. 1 illustrates the presence of indicators that reveal flaws during the process of 3D printing a product. Nevertheless, the efficiency of the process can be enhanced by integrating real-time problem detection, which might result in increased or decreased printer speed, hence reducing wastage. Hence, there is an urgent requirement for sophisticated defect detection systems that can function with utmost accuracy and effectiveness [3]. This paper introduces SurfaceVision, an advanced module developed for the automatic detection of surface defects in 3D printed objects.

The primary challenge in surface fault detection for 3D printed products that we aimed to address is the need for layer-by-layer inspection. Given that the 3D printing process involves layer by layer deposition, these defects can manifest in separate layers and need to be crucially identified. As discussed, the traditional methods are not flexible enough to analyse such accumulated defects [2]. Apart from layer by layer accumulation of these defects, the defect types, sizes and shapes can vary widely. Thus, it is challenging to create a universal fault detection system which can accurately identify all types of defects [4]. From a machine learning perspective, we aim to minimise the high false positive and false negative rates. Due to inefficient fault detection by traditional methods, such systems are not efficient enough to achieve optimum performance [3]. The last and the least challenge is the time and computational constraint put on such systems and given the large size of image data being input into these models, real time fault detection requires very high computational efficiency [1].

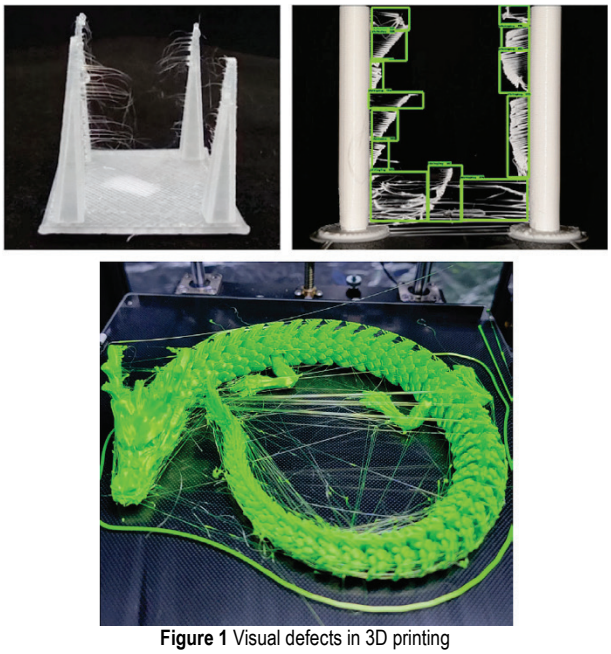

Figure 1 Visual defects in 3D printing

To address these challenges, this study introduces SurfaceVision, an advanced computer vision based fault detection module for 3D printed products. Using a

contrastive learning-based approach with a backbone of ResNet-18, SurfaceVision offers real-time, layer-wise fault detection and achieves superior accuracy with low false positive rates (FPR) and false negative rates (FNR) than the traditional methods. The proposed methodology is also computationally inexpensive and allows fast, real-time fault detection and can thus be seamlessly integrated with the manufacturing environments for Fused Deposition Modelling (FDM) processes.

The proposed framework with ResNet backbone is comprehensively evaluated against various traditional machine learning methods and other pre-trained models, demonstrating superior performance and efficiency.

2 LITERATURE REVIEW

Numerous defect detection techniques have been put forth and used over time, each with advantages and disadvantages. Traditional visual inspection and non-destructive testing methods are covered as well as more current computer-aided and machine learning-based approaches. But each of these strategies has its own set of drawbacks and difficulties. Many struggles with precisely determining the source of the problem or addressing new, unseen sorts of flaws. Some are labour-intensive; others call for specialized equipment; still others demand training or specialized equipment [7, 8]. A wide range of defect kinds, sizes, and origins must be handled by strong, scalable, and flexible defect detection algorithms in order to keep up with the rising demand for 3D printed goods. This thorough review is intended to achieve that goal. This review acts as a foundation for developing and implementing new machine learning-based approaches for defect detection, through a critical analysis of the latest advancements in defect detection methods for 3D printing [9].

A study by Chacon et al. [10] shows that build orientation does not matter if the thickness layer is increased and it also has very little effect of the edges as well. Other noteworthy results show that structural parameters have influenced mechanical properties than the actual process of the AM. Thus, the material has a different set of properties to be followed when looking at the build structure and looking for faults. Therefore, according to the findings, there are certain factors that are to be monitored while looking for faults in the AM process. The consistent monitoring approach for fault detection is valuable in studies involving multiple parameters, but its effectiveness is often obscured by the complex interplay of numerous variables and uncertainties inherent in the process. A consistent and standardized testing methodology is clearly required in Additive Manufacturing (AM), as indicated by an analysis of existing experimental studies. Accurate modelling of actual prints necessitates a thorough characterization of the process, including building parameters and boundary conditions, to adequately represent the variability within the printed parts. Additionally, there is a significant lack of research on the mechanical properties of fused parts, especially those with low densities when exposed to different types of loadings [11].

Dealing with small-scale faults or complicated geometries that might not be readily evident to the human eye might make consistent and accurate identification difficult. Additionally, the procedure is labour- and time-intensive, which reduces overall production efficiency, particularly in large- or mass-production environments [12, 13]. One of the key techniques used for such comparisons is the Hausdorff Distance, which calculates the maximum distance from a point in one set to the closest point in another set. This method is often employed to evaluate the similarity between two sets of points, such as the vertices of two meshes. The formula is defined as:

$$H(A, B) = \max\left(h(A, B), h(B, A)\right), \tag{1}$$

where $h(A, B) = h(A, B) = \max\limits_{\{a\in A\}} \min\limits_{\{b\in B\}} \| a-b \|$ and $\| a-b \|$ is the distance between points a and b.

Another method being used is the Mean Squared Error between the surfaces of the printed object and the design model can be used to quantify the error:

$$\left[MSE = \frac{2}{n} \sum_{\{i=1\}}^{\{n\}} \left(D_{\{pi\}} - D_{\{oi\}} \right)^2 \right] \tag{2}$$

where $D_{\{pi\}}$ is the distance from a point on the printed object's surface to the nearest point on the design model's surface, $D_{\{oi\}}$ is the distance from the corresponding point on the original model to the printed object. Here, n refers to the total number of points considered.

Zhang et al. [14] created a vision system that recorded sequential PBF images. Melt pool, plume, and splatter detection was their priority. Knowing the physical mechanisms behind these items helped extract their features. Support Vector Machine (SVM) classification using these characteristics yielded 90.1% quality level classification accuracy. CNNs also showed 92.7% accuracy in real-time monitoring. Many AM researchers have adapted the CNN model to address specific issues. Caggiano et al. [15] improved Selective Laser Melting (SLM) defect identification with a hierarchical deep CNN (DCNN). Scime and Beuth [16] created the multi-scale CNN (MsCNN), which improved CNN anomaly detection flexibility and classification accuracy. These models work for various materials and AM methods.

Some researchers have added image-based monitoring to control techniques. Wang et al. [17] used neural networks and vision to detect droplet phenomena in LMJP. A neural network model enabled real-time modifications, stabilizing jetting. Jin et al. [18] employed a CNN classification model to monitor and rectify Fused Deposition Modeling (FDM) processes in real time. In part quality prediction, the system has over 98% accuracy and fast defect detection and rectification.

While numerous machine learning models have been used for defect detection and monitoring in additive manufacturing (AM) via images, CNN-based models typically surpass traditional methods, providing superior

outcomes. To address this gap, Yao et al. introduced a hybrid machine learning method for recommending AM design features during the conceptual design stage. They classified design knowledge into categories such as "loadings," "objectives," and "properties," encoding them numerically and storing them in a database. Hierarchical clustering was employed to identify the correlations between design features and target features. The results were refined using a support vector machine (SVM)-based progressive dendrogram cutting technique, allowing for the identification of optimal AM design features. This approach was particularly beneficial for less experienced designers. Furthermore, various machine learning techniques, including SVM and neural networks, have been applied to enhance part design in AM processes.

Table 1 Summary of Literature Survey

Ref	Feature/Defects	ML Technique	Comment / Type of Sensors
7	Detection of Error in Fusion Ratio	KNN, SVM and MLR	90%
8	Defects at Surface Level	CNN	98%
9	Prediction Rate of Warping	SVM	97% Laser Sensor Utilized
10	Levels of Extrusion	CNN	97%
11	Identification of Surface Defects such as Cracking, Shrinkage, Stress Build-up	Ensemble of SVM and KNN	96.6%
12	Errors of Spaghetti shape	CNN	90%
13	Quality Control	Sequential CNN LSTM Ensemble	95%
14	Geometrical Defects Identification	DCNN employing transformers	97% 3D Scanner utilized
15	Misconfiguration of the shapes	YOLOv4 based outline detection	91%
16	Roughness protrusion	Semi-Supervised CNN	75%
17	Abrasion	R-CNN	98% Optical Camera
18	Defects in Layers	AutoGAN	87%
19	Surface Warps	CNN AutoEncoder	85%
20	Surface Porosity	3D Reconstruction	75%
21	Surface Roughness	YOLOv8	85%
22	Instability Prediction	SVM	85% High Speed Camera
23	Protrusion	CNN	88% NIR Camera

Zhu et al. [19] used machine learning to simulate in-plane deviations and random local variations. By creating a mathematical link between the intended and final shapes, they successfully captured global trends in shape deviation. A Gaussian process (GP) learning process is utilised to manage complex, varied data achieving an accuracy of 90%. Ferreira et al. [20] introduced a method a transfer learning and Bayesian neural networks (BNN) based method for automated geometric form deviation modelling where Geometric shapes were expressed using polar coordinates, and statistical models were applied to account for in-plane and out-of-plane deviations in shapes and processes.

Tootooni [21] applied spectral graph theory combined with machine learning to classify dimensional variations in additive manufacturing products. Spectral graph Laplacian eigenvalues derived from 3D point cloud data were utilized within machine learning models to aid classification, significantly reducing the need for post-process quality assurance. Shen [22] introduced a CNN-based framework for correcting shape deviations in additive manufacturing, where deformation features were captured by feeding a binary probabilistic distribution of the 3D model into the CNN. Inverse function networks were then trained to produce a compensated model, effectively addressing shape deviations in AM.

Khanzadeh et al. [23] used self-organizing maps (SOMs) to analyse 2D melt pool images, detecting abnormalities in thin walls manufactured using Directed Energy Deposition (DED). Based on this work, Khanzadeh et al. [23] developed a real-time porosity prediction system based on melt pool boundary morphology. To predict porosity, supervised machine learning models like k-NN, SVM, decision trees (DT), and discriminant analysis (DA) were trained using functional principal component analysis (FPCA) features derived from melt pool boundaries. Experimental results indicated that the k-NN model performed best in predicting abnormal melt pools, achieving 98.44% accuracy, while the DT model had the lowest false-negative rate at 0.033%.

3 METHODOLOGY

The key functionality of SurfaceVision is to leverage the 2D images input and identify the structural defects consisting of porous surfaces, holes detection and protrusions. The overall system can be visualized in Fig. 2. The process initiates with video data being sent via camera transmitted wirelessly. The data goes under a series of pre-processing steps, starting with resizing to a fixed dimension to maintain consistency, cropping of the object boundary and rotation correction. This is followed by the process of windowing, where continuous video data is segmented into manageable chucks, frame conversion, which standardizes the positional reference to maintain consistency in detecting surface defects. The pre-processed data is then sent to the local model, designed to interpret and recognize specific defects from the converted 2D images.

3.1 Dataset Collection and Pre-processing

To develop and evaluate the SurfaceVision module, a comprehensive dataset of 3D printed product images was collected. The dataset includes images of both defect-free and defective samples, covering a wide range of potential surface faults such as layer misalignment, incomplete layers, and surface roughness. The images were annotated by three experts, marking the presence and types of defects. This labelled dataset forms the ground truth for training and evaluation. Three independent volunteers annotated the recorded ground truth videos. Annotators' agreements were assessed using Cohen's kappa statistic, yielding a kappa value of 0.8, indicating good to substantial agreement.

The collected data can be visualized with the help of Fig. 2. Apart from the inhouse dataset, the proposed model is also trained and tested on public dataset named, 3D-Printer Defected Dataset [31], Dataset for training a model to detect anomalies during printing process. This project mainly consists of two components – defected and correct images.

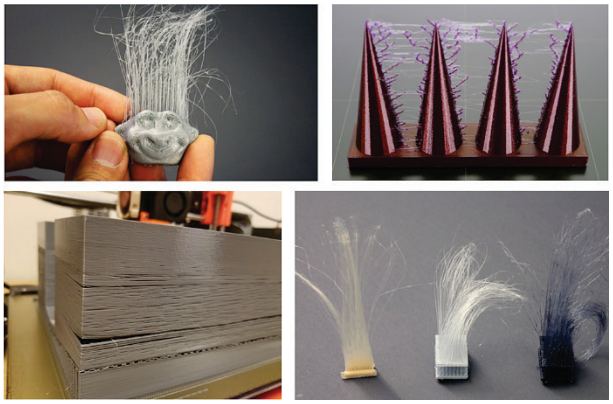

Figure 2 Dataset Visualized: Visual representation of the dataset used in the study, showcasing various types of defects in 3D printed products. The images illustrate common issues such as stringing, layer misalignment, and surface roughness, which are critical for training and evaluating the SurfaceVision module for accurate defect detection.

3.2 Model Architecture

The core of the SurfaceVision module is based on the Contrastive Learning utilizing the ResNet-18 architecture, which is well-regarded for its efficiency and accuracy in image classification tasks. There are three major classes on which the model is trained for, namely, (i) layer misalignment, (ii) incomplete layers, and (ii) surface roughness. Training and evaluation of the model were conducted on an Apple M2 Pro with 16 GB of RAM, using categorical NTXent loss and optimized with the Adam optimizer, with a learning rate initially set at 1e-4.

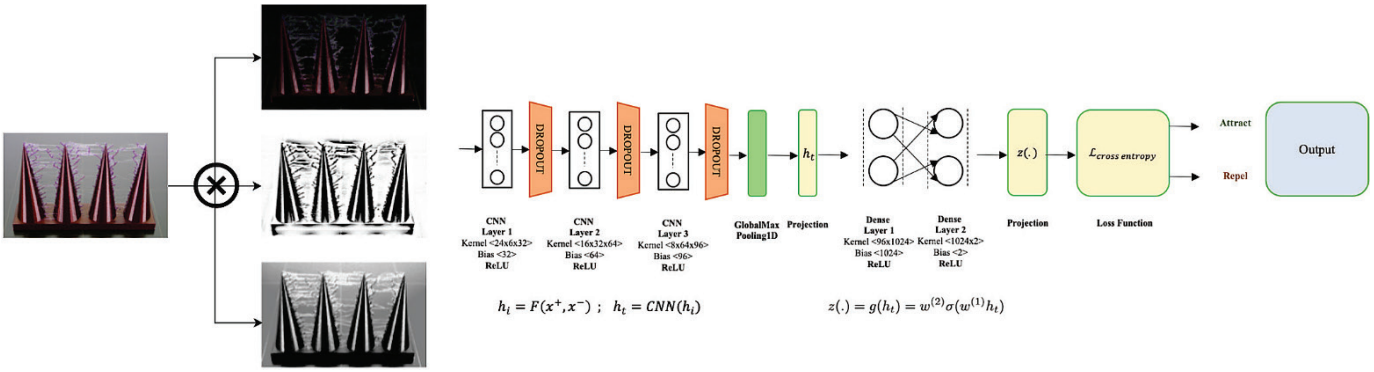

Figure 3 Proposed Network: Diagram of the proposed network architecture for SurfaceVision. The process begins with input images of 3D printed objects, which undergo various transformations and are fed into a Convolutional Neural Network (CNN) with multiple layers and dropout for regularization. The features are then pooled using Global Max Pooling and projected into a dense layer. The model is trained using a cross-entropy loss function to distinguish between defect-free and defective samples. The network aims to attract similar representations and repel dissimilar ones, resulting in an output that accurately identifies surface faults.

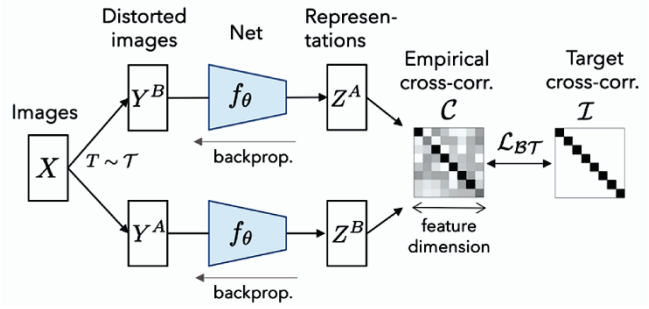

Figure 4 Contrastive Learning: Diagram illustrating the contrastive learning approach used in the SurfaceVision module. The process begins with original images X that undergo random transformations T. These transformed images Y^A and Y^B are then passed through the neural network f_θ, producing representations Z^A and Z^B. The empirical cross-correlation matrix $\boldsymbol{C}$ is computed and compared against the target cross-correlation matrix $\boldsymbol{I}$ using the loss function L_{BT}. This training process helps the model learn robust and invariant features for accurate surface fault detection [24].

Contrastive Learning: Contrastive learning a supervised learning method wherein data is distributed into positive (similar) and negative (dissimilar) pairs and the model learns by contrasting between these positive and negative pairs [5]. Concerning surface fault detection for 3D printed objects, this approach is particularly advantageous as it can group surface which are faulty with the normal ones [24]. By contrastively training a fault detection model, we can ensure that the learned representations can capture the nuanced variations and patterns in the image input leading to more accuracy. Thus, in our proposed model SurfaceVision, we employ contrastive learning wherein the loss function is supposed to minimise the distance between anchor-positive pairs and maximise the distance between anchor-negative pairs. This makes our model generalisable variations in fault manifestation, printing quality and environmental factors, ultimately enhancing the model's performance, ensuring better quality control [24].

Transformation Module, the main goal of the transformation module is to strengthen the model's capacity to learn robust and invariant features. By exposing the model to different augmented versions of the same image, the transformation module helps the network generalize better and become more resilient to variations and distortions in the input data. This is particularly important in the context of surface fault detection, where defects can manifest in various forms and scales [29]. Transformations applied in current setting:

(i) *Random Cropping*: Randomly crops a portion of the image to focus on different parts of the surface, ensuring the model learns to identify defects from partial views. Given an input image I of size $H \times W$: Randomly select a cropping window size $h \times w$, where $h < H$ and $w < W$. Randomly select the top-left corner (i, j) of the cropping window such that $0 \leq i \leq H - h$ and $0 \leq j \leq W - w$. Extract the cropped image I': $I' = I[i : i + h, j : j + w]$ [25].

(ii) *Horizontal and Vertical Flipping:* The image is flipped along the horizontal and/or vertical axis to augment the dataset, aiding the model in learning orientation-invariant features. [28]. Let horizontal flipping be I'_h

$$I'_h(i,j) = I\left(i, W - 1 - j\right). \tag{3}$$

Let vertical flipping be I'_v

$$I'_v(i,j) = I\left(H - 1 - i, j\right). \tag{4}$$

(iii) *Gaussian Blurring:* Adds Gaussian blur to the image to simulate surface texture variations and imperfections. Given an input image I and a Gaussian kernel G [29]: 1. Apply the Gaussian filter to the image:

$$I' = I * G, \tag{5}$$

where $*$ denotes the convolution operation. These transformations help in augmenting the dataset and improving the model's ability to generalize and become more resilient to variations and distortions in the input data. The output of the transformation module is fed to the base model [29].

(iv) *Rotation:* Rotates the image by a random angle to simulate different printing orientations and perspectives. Given an input image I and a rotation angle θ [29]: 1. Compute the transformation matrix $\boldsymbol{T}$:

$$\boldsymbol{T} = \begin{bmatrix} \cos(\theta) & -\sin(\theta) & 0 \\ \sin(\theta) & \cos(\theta) & 0 \\ 0 & 0 & 1 \end{bmatrix}. \tag{6}$$

Applying the rotation transformation to each pixel (x, y) in the image give the following outcome:

$$\begin{bmatrix} x' \\ y' \\ 1 \end{bmatrix} = \boldsymbol{T} \begin{bmatrix} x \\ y \\ 1 \end{bmatrix}. \tag{7}$$

(v) *Color Jittering:* Applies random changes to the brightness, contrast, saturation, and hue of the image to improve the model's robustness to lighting variations. Given an input image I and random changes for brightness Δ_b, contrast Δ_c, saturation Δ_s, and hue Δ_h: 1 [26].

Brightness Δ_b:

$$I' = I + \Delta_b, \tag{8}$$

Contrast Δ_c:

$$I' = I \cdot \Delta_c, \tag{9}$$

Saturation Δ_s:

$$I'_{HSV}(i,j,1) = I_{HSV}(i,j,1) \cdot \Delta_s, \tag{10}$$

Hue Δ_h:

$$I'_{HSV}(i,j,0) = I_{HSV}(i,j,0) + \Delta_h. \tag{11}$$

(vi) *Scaling and Resizing:* Scales the image up or down and resizes it to a fixed dimension to ensure uniform input size while preserving important features. Given an input image I and a scaling factor s: 1 [28]

$$I' = \text{resize}(I, s \cdot H, s \cdot W). \tag{12}$$

Resize the image to a fixed size $H' \times W'$:

$$I' = \text{resize}(I, H', W'). \tag{13}$$

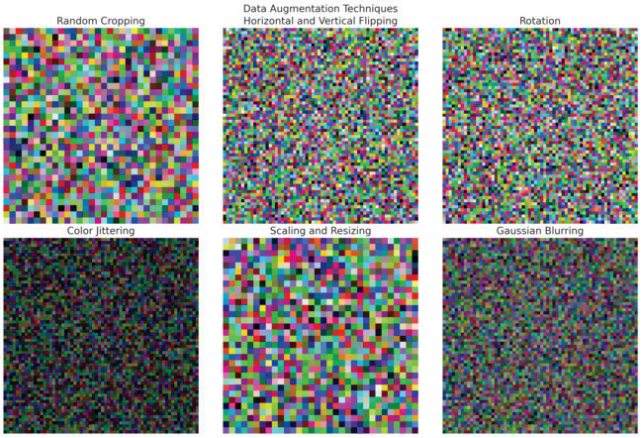

Figure 5 Visualization of various data augmentation techniques applied to the dataset, including random cropping, horizontal and vertical flipping, rotation, color jittering, scaling and resizing, and Gaussian blurring. These augmentations increase dataset diversity and model robustness.

Base Model. This model features 18 layers with residual blocks designed to alleviate the vanishing gradient issue, enabling the training of deeper networks. The architecture is initialized with weights pre-trained on the ImageNet dataset. In this context, x denotes the input to the residual block, $(\{W_i\})$ represents the residual function (typically a combination of convolutions, batch normalization, and ReLU activations), and y is the output of the residual block. During training, a forward pass is performed where a batch of images—including anchor, positive, and negative samples—are processed through the modified ResNet-18 to obtain embedding.

Loss Function. Contrastive loss is determined by evaluating the distance between anchor-positive and anchor-negative pairs, and this function is applied across the batch to calculate the total loss. The objective of contrastive learning is to create an embedding space where similar samples are clustered closer together, while dissimilar samples are pushed further apart. Common contrastive loss techniques include triplet loss and contrastive loss [30]. For simplicity, we will use the contrastive loss:

$$\mathcal{L} = \frac{1}{N}\sum_{i=1}^{N}\left[y_i \times D^2(h_i, h_i^+) + (1-y_i)\times \max\left(0, m - D(h_i, h_i^-)\right)^2 \right]. \quad (14)$$

Where, N is the number of samples, y_i is a binary label indicating whether the pair (h_i, h_i^+) is similar (y_i = 1) or dissimilar (y_i = 0). h_i is the embedding of the anchor sample. h_i^+ is the embedding of the positive sample (similar to the anchor). h_i^- is the embedding of the negative sample (dissimilar to the anchor). $D(.,.)$ is a distance metric (typically Euclidean distance). m is a margin parameter that ensures dissimilar pairs are at least m units apart. Next, backpropagation is performed to compute gradients. The network parameters are updated using an optimizer (e.g. Adam). The pre-trained ResNet-18 model was fine-tuned using our 3D printing dataset. This process involved replacing the final fully connected layer with a new layer specifically designed for our classification task, distinguishing between defect types and no defects.

4 RESULTS AND ANALYSIS

This section provides a comprehensive performance analysis of SurfaceVision in comparison to the state-of-the-art methods. It also expands on the design rationale behind various components, offering deeper insights into their development.

4.1 Experimental Protocol and Evaluation Metrics

The in-house dataset is divided into training, testing, and validation sets with a 70:20:10 split ratio. The training and evaluation are conducted on a Tesla V100-DGXS GPU with 32 GB of memory, over 50 epochs, divided into five distinct phases. The best-performing model from each phase progresses to the next, ensuring a gradual refinement of parameters and optimization of performance. Cross Entropy Loss, which is well-suited for multi-class classification, is employed, and training is optimized using the Adam optimizer with a learning rate of 5×10^{-5}.

During dataset analysis, an imbalance was observed, with fewer instances of the non-target class. Since the model's performance depends on both precision and recall, the macro F1 score was deemed the most suitable evaluation metric. Variations and noise in the dataset skew the performance to the majority class which is not desirable in order to achieve fewer false positive rates.

The evaluation metrics used in this study to analyse the performance of SurfaceVision include Accuracy, Precision, Recall, F1-Score, and Evaluation Time. Here are the formulas for these metrics:

$$Accuracy = TP + \frac{TN}{TP + TN + FP + FN}, \quad (15)$$

where: TP = True Positives, TN = True Negatives, FP = False Positives, N = False Negatives.

$$Precision = \frac{TP}{TP + FP}. \quad (16)$$

Precision measures the ratio of true positive to all positive predictions made by the model.

$$Recall = \frac{TP}{TP + FN}. \quad (17)$$

Recall measures the ratio of true positive predictions to all actual positive cases in the dataset.

$$F1\text{-}Score = 2 \times \frac{Precision \times Recall}{Precision + Recall}. \quad (18)$$

The $F1$-$Score$ is the harmonic mean of Precision and Recall, providing a single metric that balances both metrics. Inference time measures the average time taken by the model to make a prediction for a single input sample, measured in milliseconds (ms).

4.2 Experiment 1: Baselining and Independent Attribute Analysis

The two primary objectives of this study are: 1) To standardise and validate domain knowledge on surface anomalies attributing to defects 2) To identify newer surface attributes for fault detection and localisation. In Tab. 2, we compared SurfaceVision's performance against several baseline algorithms including Support Vector Machines (SVM), Random Forests, AlexNet and VGG16. The results conclude that our ResNet18 based SurfaceVision model outperforms these baseline algorithms achieving superior accuracy and computational efficiency with an average increase of 12-20%.

In Tab. 2, initial baseline experiments on the dataset confirmed that the multimodal approach, combining both surface texture and structural integrity features, outperforms the use of individual modalities. The combination of ResNet-18 for texture analysis and a custom Contrastive Network for structural feature extraction yielded the best results and was therefore used for all subsequent experiments and analyses.

To assess the impact of individual surface attributes, we conducted ablation studies by masking one attribute at a time from either the texture or structural components, while keeping the other components unmasked. This approach

allowed us to understand the comparative impact of specific surface attributes on defect detection accuracy, while maintaining consistent conditions for other factors. The analysis, Fig. 7, reveals that attributes such as 'layer consistency', 'surface smoothness', and 'edge sharpness' provide the best overall performance as individual surface attributes. These attributes can potentially be used in isolation for training and validation purposes.

Table 2 Classification Results

Algorithm	Accuracy (%)	Precision (%)	Recall (%)	F1-Score (%)	Inference Time (ms)
Support Vector Machines (SVM)	75.4	72.3	70.5	71.4	15.3
Random Forests	78.9	76.1	74.8	75.4	20.7
AlexNet	82.3	80.4	79.1	79.7	25.4
VGG16	84.1	82.7	81.3	82	30.1
SurfaceVision (Custom Contrastive Network)	91.5	90.2	89.4	89.8	12.5

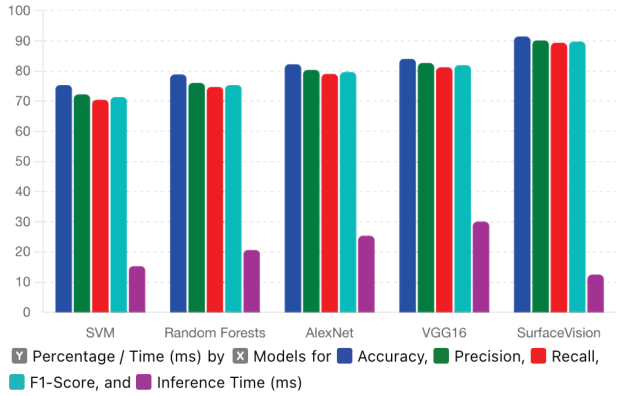

Figure 6 Comparison of performance metrics (Accuracy, Precision, Recall, F1-Score, and Inference Time) across different models (SVM, Random Forests, AlexNet, VGG16, SurfaceVision). SurfaceVision demonstrates superior performance in all metrics.

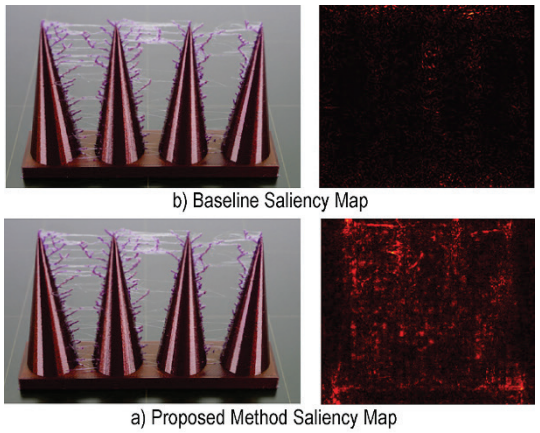

Figure 7 Comparison of proposed method (b) v/s baseline methods (a) by generating the saliency maps. SurfaceVision utilizes a hierarchical parsing-driven attention mechanism, resulting in more focused and precise areas of interest, which enhances defect detection.

The baseline method, shown in Fig. 7b, exhibits dispersed and unfocused attention, highlighting non-critical areas of the 3D printed surface. This can result in higher false positives and false negatives, as the model struggles to isolate relevant defects. In contrast, the proposed method, displayed in Fig. 7a, utilizes a hierarchical parsing-driven attention mechanism that sharply focuses on critical regions of interest, such as the protrusions caused by stringing errors. The precise localization and improved saliency provided by SurfaceVision ensure enhanced defect detection accuracy, which is particularly crucial for identifying intricate surface-level faults like layer misalignment or material inconsistencies. Furthermore, this focused approach can be adapted to other defect scenarios, such as delamination of layers, as the hierarchical attention mechanism is capable of capturing structural discontinuities in the printed material. This adaptability emphasizes the robustness and versatility of the SurfaceVision framework.

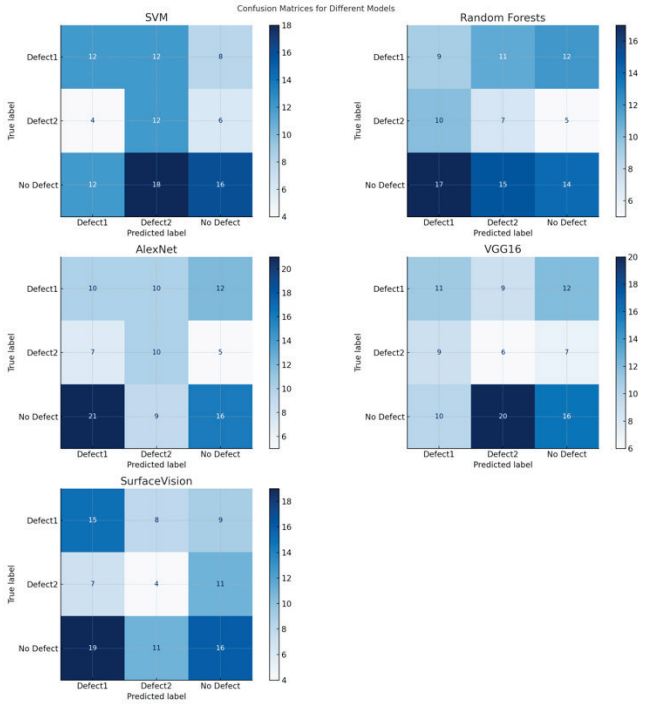

Figure 8 Confusion matrices for different models (SVM, Random Forests, AlexNet, VGG16, SurfaceVision) showing the classification performance for defect types. SurfaceVision exhibits the fewest misclassifications.

The confusion matrices, Fig. 8, provide a detailed view of the classification performance of each model for different defect types:

SVM: Struggles with distinguishing between 'Defect1' and 'Defect2'. Misclassifies 'No Defect' instances more frequently compared to other models.

Random Forests: Shows better performance than SVM in some categories but still has significant misclassifications. Has trouble distinguishing between 'Defect1' and 'Defect2'.

AlexNet: Shows improvement in classifying 'No Defect' but still misclassifies a substantial number of 'Defect1' and 'Defect2'. Better performance compared to SVM and Random Forests.

VGG16: Better at distinguishing between 'Defect1', 'Defect2', and 'No Defect'. Misclassifications are fewer compared to SVM, Random Forests, and AlexNet.

SurfaceVision: Exhibits the best performance among all models. Fewest misclassifications for all defect types, indicating high precision and recall.

For the inhouse dataset, most individual surface attributes demonstrated sub-par performance compared to the multimodal architecture during baseline testing. This suggests their potential to be used as sole indicators of defects in AI-based and non-AI-based quality control interventions. The performance metrics for the industrial dataset are notably lower than those for in house, reflecting challenges associated with lower variability and smaller sample sizes.

Despite this, many surface attributes such as 'layer consistency', 'surface smoothness', 'edge sharpness', and 'layer adhesion' show high diagnostic efficiency even in settings with limited sample sizes. This highlights the robustness of these attributes in real-world defect detection scenarios.

4.3 Experiment 2: Visualization of the Classification Decisions Using Semantic Maps

Using saliency maps to visualize the classification decisions of models techniques provides valuable insights into how the models prioritise and interpret various surface variables during their learning process. Fig. 4 illustrates the comparison of saliency maps for both methodologies. When comparing our methodology with the baseline model, we saw that the model has significantly improved by using a hierarchical parsing-driven attention mechanism. Both techniques enhance the sharpness of the area of interest in structural images compared to the baseline method. In the baseline method, the attention is distributed to non-critical areas that are typically not suggestive of faults, as shown in Fig. 4.

The saliency maps comparison highlights the differences in how baseline models and SurfaceVision prioritize and interpret various surface features: Baseline Models: Tend to distribute attention to non-critical areas. Show less focused and broader areas of interest, which might lead to higher false positives and negatives. SurfaceVision: Utilizes a hierarchical parsing-driven attention mechanism, resulting in more focused and precise areas of interest. Targets critical surface features more effectively, which contributes to its superior performance in defect detection.

5 LIMITATIONS AND FUTURE WORK

The current SurfaceVision system relies on an optical camera, which inherently limits fault detection to regions within the camera's field of view. While this setup is effective for surface-level defect detection, it cannot capture errors in hidden zones or on the back of the model. To overcome this limitation, potential upgrades to the system could include integrating a multi-camera setup to provide 360-degree coverage of the object or employing robotic arms equipped with cameras to dynamically inspect all sides of the model. Additionally, non-visual sensing techniques, such as ultrasonic testing, thermal imaging, or infrared cameras, could complement the optical system by detecting structural and thermal inconsistencies in areas that are not directly visible. These enhancements would significantly improve the system's comprehensiveness and make it suitable for more complex or intricate 3D-printed models. Incorporating such advanced techniques into SurfaceVision is proposed as a future direction for extending its application scope and robustness.

6 CONCLUSION

This study presented SurfaceVision, an automated system for real-time surface fault detection in 3D-printed products, leveraging the ResNet-18 architecture and contrastive learning. The system demonstrated better performance compared to traditional machine learning methods and pre-trained models, achieving a 91.5% accuracy with significantly reduced inference times. By employing a hierarchical parsing-driven attention mechanism, SurfaceVision effectively localized critical defects, such as layer misalignment, surface roughness, and incomplete layers, as evidenced by the referenced saliency maps. Compared to prior works, such as SVM-based approaches with limited generalization or CNN methods lacking real-time efficiency, SurfaceVision excels in both adaptability and precision, with an average improvement of 12-20% in key metrics. While the system currently detects only visible surface faults within the camera's field of view, future enhancements could include multi-camera setups, robotic inspection systems, and non-visual modalities like thermal or ultrasonic imaging to cover hidden zones and internal defects. These results underscore the potential of SurfaceVision to significantly improve quality control in additive manufacturing, offering a scalable and efficient solution for reducing waste and enhancing product reliability. By addressing current limitations and broadening its scope to more complex defect scenarios, SurfaceVision could further solidify its role in Industry 4.0 workflows.

7 REFERENCES

[1] Ford, S. (2014). Additive manufacturing technology: Potential implications for U.S. manufacturing. *Journal of Industrial Technology, 30*(4), 1-15.

[2] Gibson, I., Rosen, D. & Stucker, B. (2015). *Additive manufacturing technologies: 3D printing, rapid prototyping, and direct digital manufacturing*. Springer. https://doi.org/10.1007/978-1-4939-2113-3

[3] Huang, Y., Liu, W., Mokasdar, A. & Hou, L. (2013). Additive manufacturing and its societal impact: A literature review. *The International Journal of Advanced Manufacturing Technology, 67*(5-8), 1191-1203. https://doi.org/10.1007/s00170-012-4558-5

[4] Villarrubia, J. S. (2012). Algorithms for automated inspection of 3D printed parts. *Precision Engineering, 36*(4), 614-628.

[5] Chen, T., Kornblith, S., Norouzi, M. & Hinton, G. (2020). A simple framework for contrastive learning of visual representations. In *International conference on machine learning (ICML2020)*, 1597-1607.

[6] He, K., Zhang, X., Ren, S. & Sun, J. (2016). Deep residual learning for image recognition. In *Proceedings of the IEEE*

conference on computer vision and pattern recognition, 770-778. https://doi.org/10.1109/CVPR.2016.90

[7] Fu, Y., Downey, A. R., Yuan, L., Zhang, T., Pratt, A. & Balogun, Y. (2022). Machine learning algorithms for defect detection in metal laser-based additive manufacturing: A review. *Journal of Manufacturing Processes, 75*, 693-710. https://doi.org/10.1016/j.jmapro.2021.12.061

[8] Wu, Y., Fang, J., Wu, C., Li, C., Sun, G. & Li, Q. (2023). Additively manufactured materials and structures: A state-of-the-art review on their mechanical characteristics and energy absorption. *International Journal of Mechanical Sciences*, 108102. https://doi.org/10.1016/j.ijmecsci.2023.108102

[9] Leach, R., Carmignato, S., Dewulf, W., Doradi, M. & Van Veghel, J. (2020). Precision additive manufacturing. *CIRP Annals, 69*(2), 710-733. https://doi.org/10.1201/9780429436543

[10] Ferrando Chacon, J. L. (2015). Fault detection in rotating machinery using acoustic emission. *Doctoral dissertation*, Brunel University London.

[11] Mirzaei, K., Arashpour, M., Asadi, E., Masoumi, H., Bai, Y. & Behnood, A. (2022). 3D point cloud data processing with machine learning for construction and infrastructure applications: A comprehensive review. *Advanced Engineering Informatics, 51*, 101501. https://doi.org/10.1016/j.aei.2021.101501

[12] Parmar, H., Khan, T., Tucci, F., Umer, R. & Carlone, P. (2022). Advanced robotics and additive manufacturing of composites: towards a new era in Industry 4.0. *Materials and manufacturing processes, 37*(5), 483-517. https://doi.org/10.1080/10426914.2020.1866195

[13] Akhavan, J. & Manoochehri, S. (2022, June). Sensory data fusion using machine learning methods for in-situ defect registration in additive manufacturing: a review. In *IEEE International IOT, Electronics and Mechatronics Conference (IEMTRONICS2022)*, 1-10. https://doi.org/10.1109/IEMTRONICS55184.2022.9795815

[14] Zhang, H., Vallabh, C. K. P. & Zhao, X. (2023). Machine learning enhanced high dynamic range fringe projection profilometry for in-situ layer-wise surface topography measurement during LPBF additive manufacturing. *Precision Engineering, 84*, 1-14. https://doi.org/10.1016/j.precisioneng.2023.06.015

[15] Wegener, K., Spierings, A. B., Teti, R., Caggiano, A., Knüttel, D., & Staub, A. (2021). A conceptual vision for a bio-intelligent manufacturing cell for Selective Laser Melting. *CIRP Journal of Manufacturing Science and Technology, 34*, 61-83. https://doi.org/10.1016/j.cirpj.2020.11.009

[16] Scime, L. & Beuth, J. (2019). Using machine learning to identify in-situ melt pool signatures indicative of flaw formation in a laser powder bed fusion additive manufacturing process. *Additive Manufacturing, 25*, 151-165. https://doi.org/10.1016/j.addma.2018.11.010

[17] Wang, C., Tan, X. P., Tor, S. B. & Lim, C. S. (2020). Machine learning in additive manufacturing: State-of-the-art and perspectives. *Additive Manufacturing, 36*, 101538. https://doi.org/10.1016/j.addma.2020.101538

[18] Li, R., Jin, M. & Paquit, V. C. (2021). Geometrical defect detection for additive manufacturing with machine learning models. *Materials & Design, 206*, 109726. https://doi.org/10.1016/j.matdes.2021.109726

[19] Zhu, Q., Liu, Z. & Yan, J. (2021). Machine learning for metal additive manufacturing: predicting temperature and melt pool fluid dynamics using physics-informed neural networks. *Computational Mechanics, 67*, 619-635. https://doi.org/10.1007/s00466-020-01952-9

[20] Ferreira, R. D. S. B., Sabbaghi, A. & Huang, Q. (2019). Automated geometric shape deviation modeling for additive manufacturing systems via Bayesian neural networks. *IEEE Transactions on Automation Science and Engineering, 17*(2), 584-598. https://doi.org/10.1109/TASE.2019.2936821

[21] Samie Tootooni, M., Dsouza, A., Donovan, R., Rao, P. K., Kong, Z. & Borgesen, P. (2017). Classifying the dimensional variation in additive manufactured parts from laser-scanned three-dimensional point cloud data using machine learning approaches. *Journal of Manufacturing Science and Engineering, 139*(9), 091005. https://doi.org/10.1115/1.4036641

[22] Yuan, S., Shen, F., Chua, C. K. & Zhou, K. (2019). Polymeric composites for powder-based additive manufacturing: Materials and applications. *Progress in Polymer Science, 91*, 141-168. https://doi.org/10.1016/j.progpolymsci.2018.11.001

[23] Francis, J., Khanzadeh, M., Doude, H., Hammond, V. & Bian, L. (2019). Data-driven calibration for infrared camera in additive manufacturing. *International Journal of Rapid Manufacturing, 8*(4), 302-325. https://doi.org/10.1504/IJRAPIDM.2019.102531

[24] He, K., Zhang, X., Ren, S. & Sun, J. (2016). Deep residual learning for image recognition. In *Proceedings of the IEEE conference on computer vision and pattern recognition*, 770-778. https://doi.org/10.1109/CVPR.2016.90

[25] Goodfellow, I., Bengio, Y. & Courville, A. (2016). *Deep learning*. MIT press.

[26] Howard, A. G. (2013). Some improvements on deep convolutional neural network based image classification. *arXiv* preprint arXiv:1312.5402.

[27] Perez, L. & Wang, J. (2017). The effectiveness of data augmentation in image classification using deep learning. *arXiv* preprint arXiv:1712.04621.

[28] Shorten, C. & Khoshgoftaar, T. M. (2019). A survey on image data augmentation for deep learning. *Journal of Big Data, 6*(1), 1-48. https://doi.org/10.1186/s40537-019-0197-0

[29] Simard, P. Y., Steinkraus, D. & Platt, J. C. (2003). Best practices for convolutional neural networks applied to visual document analysis. In *Icdar, Vol. 3*, 958-962. https://doi.org/10.1109/ICDAR.2003.1227801

[30] Hadsell, R., Chopra, S. & LeCun, Y. (2006). Dimensionality reduction by learning an invariant mapping. In *IEEE Computer Society Conference on Computer Vision and Pattern Recognition (CVPR2006), Vol. 2*, 1735-1742. https://doi.org/10.1109/CVPR.2006.100

[31] Bo-Kai Ruan. (2023). 3D Printer Defected Dataset. Kaggle. https://www.kaggle.com/datasets/justin900429/3d-printer-defected-dataset

Authors' contacts:

Laukesh Kumar
(Corresponding author)
USICT, Guru Gobind Singh Indraprastha University,
Dwarka, New Delhi, Delhi 110078, India
laukeshbhati@gmail.com

Manoj Kumar Satyarthi
USICT, Guru Gobind Singh Indraprastha University,
Dwarka, New Delhi, Delhi 110078, India